



# Linking variability of monsoon precipitation with satellite-based observations of stable water isotopes over Northeast India

ROHIT PRADHAN\* , NIMISHA SINGH and RAGHAVENDRA P SINGH

Land Hydrology Division, EPSA, Space Applications Centre (ISRO), Ahmedabad 380 015, India.

\*Corresponding author. e-mail: rohitp@sac.isro.gov.in

MS received 31 May 2019; revised 9 September 2019; accepted 19 September 2019; published online 20 December 2019

Isotopic composition of atmospheric water vapor provides information on transport, mixing and phase change of water in the atmosphere. It provides a useful tool for understanding various aspects of the hydrological cycle. SCanning Imaging Absorption Spectrometer for Atmospheric CHartography (SCIAMACHY) onboard ENVISAT-1 was a spectrometer designed to measure the composition of trace gases in troposphere and stratosphere. It provided global measurements of total columnar HDO and H<sub>2</sub>O concentrations using the spectral window between 2338.5 and 2382.5 nm. Temporal variability of columnar  $\delta D$  was studied over Northeast (NE) India and mean columnar  $\delta D$  for pre-monsoon and monsoon months were correlated with precipitation data obtained from Global System for Mapping of Precipitation (GSMaP). It was observed that  $\delta D$  during the pre-monsoon months of April–May showed good correlation ( $r > 0.7$ ,  $p < 0.05$ ) with total precipitation during June–August for the corresponding year over forested regions of Meghalaya and parts of Assam. Analysis was also carried out to understand the relationship between SCIAMACHY derived gridded monthly  $\delta D$  and Multivariate El-Niño Index (MEI) with zero and one month lag periods. Positive correlation was observed between  $\delta D$  and MEI over parts of Central India, Myanmar and Thailand. Isotope ratio of water vapor provides additional information compared to traditional meteorological observations and holds the potential to improve forecasting models.

**Keywords.** Stable isotopes; SCIAMACHY; Northeast India; hydrology; ENSO.

## 1. Introduction

Study of Indian Summer Monsoon (ISM) rainfall is essential in understanding the hydrological cycle of the country (Guhathakurta and Rajeevan 2008). Northeast (NE) Indian region receives some of the heaviest rainfall during ISM (around 1400 mm) as compared to other parts of Indian subcontinent (Prabhu *et al.* 2017). This area is dominated by dynamic weather arising due to its diverse orographic conditions (Mahanta *et al.*

2013). Both local and remote forces (Prabhu *et al.* 2017) govern ISM rainfall in the eastern-most part of the country. In the last few decades, this region has experienced a decline in ISM rainfall (Preethi *et al.* 2017) leading to drought like conditions in different states of NE India. Western disturbance and Nor'westers are major phenomenon governing moisture transport over NE India during winter and pre-monsoon months, respectively (Laskar *et al.* 2015; Jeelani *et al.* 2018).

Studying isotopic composition of water vapor provides information about the history of mixing and phase change associated with a given air parcel (Dansgaard 1964; Gat 1996; Mook 2000). Isotopic analysis of precipitation has been widely used to understand moisture sources over specific regions (Deshpande *et al.* 2010; Srivastava *et al.* 2014; Lekshmy *et al.* 2015). Source of moisture during ISM over Northeastern states has been studied using stable water isotopes in rainwater samples (Breitenbach *et al.* 2010). Isotopic composition of water vapor differs with that of precipitation due to different sources and hence, remote sensing gives new information about the hydrological cycle, which is unattainable from surface (Worden *et al.* 2007). Rainfall depletes the resulting vapor, as heavier isotopes tend to condense easily. On the other hand, isotope ratios can indicate how the atmosphere is conditioned by various surface processes like evaporation and transpiration, which can in turn influence precipitation. Limited work has been carried out connecting monsoon precipitation with satellite-based observations of stable water isotopes over India.

Satellite-based remote sensing of water isotopes in atmosphere has been used to understand various hydrological processes (Worden *et al.* 2007; Frankenberg *et al.* 2009; Lee *et al.* 2012). Satellite-based sensors like SCanning Imaging Absorption Spectrometer for Atmospheric CHartographyY (SCIAMACHY), Tropospheric Emission Spectrometer (TES), Michelson Interferometer for Passive Atmospheric Sounding (MIPAS) and Atmospheric Chemistry Experiment-Fourier Transform Spectrometer (ACE-FTS) have provided isotopic ratio observations with global coverage (Worden *et al.* 2006; Nassar *et al.* 2007; Payne *et al.* 2007; Schneider *et al.* 2018). SCIAMACHY, on board ENVISAT-1 launched in March 2002, was a spectrometer designed to measure the composition of trace gases in the troposphere and stratosphere. SCIAMACHY retrieves columnar water isotope ratios of HDO/H<sub>2</sub>O using the Shortwave-Infrared Carbon Monoxide Retrieval (SICOR) algorithm (Schneider *et al.* 2018) and performs joint retrieval of CH<sub>4</sub>, H<sub>2</sub>O, HDO and CO (Scheepmaker *et al.* 2013) to reduce uncertainty. Limitations in sensitivity of current instruments restrict the retrieval of H<sub>2</sub><sup>18</sup>O; hence, observations of D/H ratio are only available from space-based platforms.

Several global climate phenomenon like El-Niño and La-Niña accompanied by atmospheric

circulations, such as El-Niño-Southern Oscillation (ENSO) and Indian Ocean Dipole (IOD), also affect the ISM rainfall variability (Krishna Kumar *et al.* 1995) resulting in drought and flood-like situations in different parts of the country (Philander 1983). Out of these, ENSO is considered an important driving factor that affects the inter-annual variations in ISM (Walker 1923). To monitor ENSO, various indices like Southern Oscillation Index (SOI), Multivariate ENSO Index (MEI), NOAA Oceanic Niño Index (ONI), etc. have been used to quantify the nature of atmosphere-ocean circulations. MEI is well suited to monitor ENSO events as compared to others, because it takes into account six variables of meteorological and oceanographic components (Wolter and Timlin 1998) over the Pacific Ocean. Studies have been carried out to establish relationship between stable water isotopes and ENSO variability in different parts of the globe. Vuille and Werner (2005) studied the relationship between South American Summer Monsoon and ENSO analyzing the stable isotopes in precipitation. Similar studies have been carried out by Okazaki *et al.* (2015) over Western Africa connecting ENSO with inter-annual variability of isotopic composition in water vapor using satellite-based observation and model simulations. However, there exists a gap area in understanding the effect of these phenomenon on the distribution of water isotope ratios in the atmosphere over Indian landmass. In this paper, we attempt to understand the relationship between water isotope ratios and monsoon precipitation over NE India during pre-monsoon and monsoon seasons. We also studied the response of atmosphere over Indian mainland in connection to ENSO events.

## 2. Study area and data used

SCIAMACHY Level-2 point retrievals of HDO and H<sub>2</sub>O for each orbit (available at [ftp://ftp.sron.nl/pub/pub/DataProducts/SCIAMACHY\\_HDO/](ftp://ftp.sron.nl/pub/pub/DataProducts/SCIAMACHY_HDO/) (Schneider *et al.* 2018)) were selected for the period 2003–2011 over Northeast India with bounding box 22°–28°N and 88°–98°E as shown in figure 1. This region comprises over 60% forest cover (Jain *et al.* 2013) along with the flood plains of Brahmaputra river in Assam and Bangladesh. Forests of NE India are regarded as the northernmost limit of tropical rainforests in the world (Procter *et al.* 1998). This region is an important

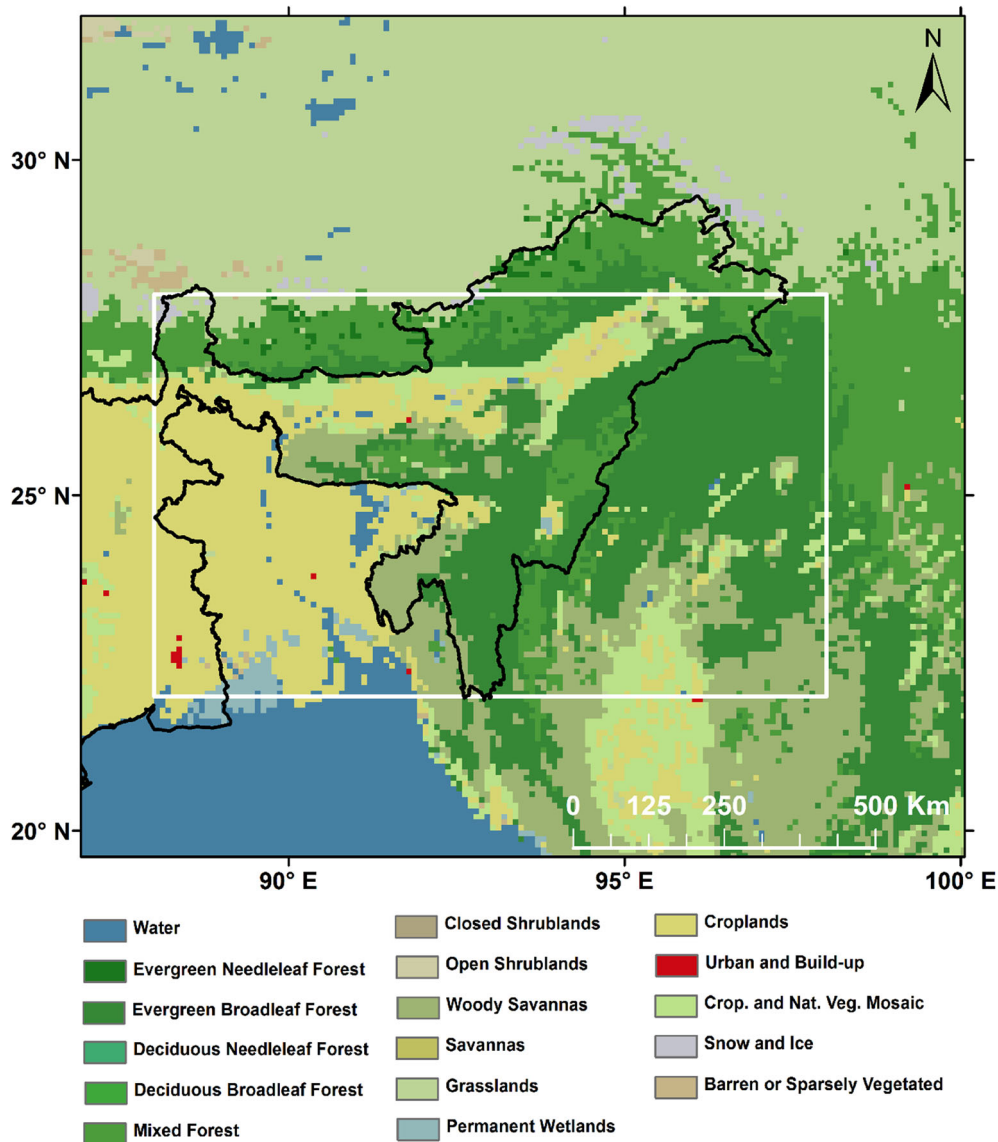


Figure 1. Study area (white bounding box) overlaid on MODIS LULC for 2009 (Friedl *et al.* 2010).

biodiversity hotspot of India and a wide variety of flora and fauna are found here (Dikshit and Dikshit 2014). The onset of ISM in the region is usually between 1 and 10 June every year (IMD Report 2009).

Precipitation data was obtained from Global System for Mapping of Precipitation (GSMaP), provided by JAXA’s Global Rainfall Watch System. Gauge calibrated GSMaP data is available at multiple spatial ( $0.1^\circ \times 0.1^\circ$  and  $0.25^\circ \times 0.25^\circ$  grids) as well as temporal scales (hourly and daily). Daily GSMaP data at spatial resolution of  $0.1^\circ \times 0.1^\circ$  was used in our study for the year 2003–2011. Multivariate El-Niño Index (MEI) data was obtained from NOAA (<https://www.esrl.noaa.gov/psd/enso/mei/>).

### 3. Methodology

Orbit-wise SCIAMACHY Level-2 retrievals of columnar HDO and H<sub>2</sub>O concentrations for the period 2003–2011 were used in this study. Individual point retrievals were filtered using the quality control criteria suggested by Schneider *et al.* (2018). Methane and water vapor being the major gases, constraints are applied on their concentration values based on *a priori* model estimates. This allows removal of spurious outliers from the data. Based on this, only those data points were considered which meet the following conditions:

$$0.9 < \frac{C_{CH_4}}{C_{CH_4+TM_5}} < 1.1, \quad (1)$$

$$0.7 < \frac{C_{\text{H}_2\text{O}}}{C_{\text{H}_2\text{O-ECMF}}}, \quad (2)$$

where,  $C_{\text{CH}_4}$  and  $C_{\text{H}_2\text{O}}$  are columnar concentrations of  $\text{CH}_4$  and  $\text{H}_2\text{O}$  and  $C_{\text{CH}_4\text{-TM5}}$  and  $C_{\text{H}_2\text{O-ECMF}}$  are corresponding model predictions of columnar concentrations. These two criteria act as simple cloud filter.  $P_{15.9}$  and  $P_{84.1}$  (15.9th and 84.1th percentile) of logarithmic HDO and  $\text{H}_2\text{O}$  data distribution (Schneider *et al.* 2018) are used to define  $\sigma$  as follows:

$$\sigma = \frac{1}{2}(P_{84.1} - P_{15.9}). \quad (3)$$

Data points with absolute error in  $\text{H}_2\text{O}$  and HDO concentrations within  $5\sigma$  around median ( $\mu_e$ ) are used. Points are also filtered on the basis of root mean square of the spectral fit residual  $c_{\text{rms}}$  keeping data only within  $6\sigma$  around median ( $\mu_{\text{rms}}$ ).

$$\mu_{e(\text{H}_2\text{O})} - 5\sigma_{e(\text{H}_2\text{O})} < \log e_{\text{H}_2\text{O}} < \mu_{e(\text{H}_2\text{O})} + 5\sigma_{e(\text{H}_2\text{O})}, \quad (4)$$

$$\mu_{e(\text{HDO})} - 5\sigma_{e(\text{HDO})} < \log e_{\text{HDO}} < \mu_{e(\text{HDO})} + 5\sigma_{e(\text{HDO})}, \quad (5)$$

$$\mu_{\text{rms}} - 6\sigma_{\text{rms}} < \log c_{\text{rms}} < \mu_{\text{rms}} + 6\sigma_{\text{rms}}. \quad (6)$$

Along with this, data points are also filtered on the basis of number of iterations performed to reach an optimum solution,  $N_{\text{iter}} \leq 12$  and observations with solar zenith angle  $v_{\text{sz}} < 70^\circ$ . These quality control criteria prevent spurious concentration observations from being used in analysis. Once the valid data points along with the day of observation are obtained, these are binned onto  $2^\circ \times 2^\circ$  grids for every 5-day period (pentad). Stable isotope ratio of  $\text{HDO}/\text{H}_2\text{O}$  is usually defined in parts per thousand (per mil—‰) relative to a standard (Vienna Standard Mean Ocean Water, VSMOW) and given by delta ( $\delta$ —notation) expressed by equation 7.

$$\delta\text{D} = \left[ \frac{(\text{HDO}/\text{H}_2\text{O})_{\text{sample}}}{(\text{HDO}/\text{H}_2\text{O})_{\text{VSMOW}}} - 1 \right] \times 1000(\text{‰}), \quad (7)$$

where the value of  $(\text{HDO}/\text{H}_2\text{O})_{\text{VSMOW}}$  is  $3.11 \times 10^{-4}$ .  $\delta\text{D}$  was computed for each valid retrieval and binned across entire study area for every pentad. These pentad-averaged total columnar  $\delta\text{D}$  were plotted to depict the temporal variability over study area and understand its seasonal cycle.

Valid observations over NE India for the year 2003–2011 across all the individual orbits were binned to calculate pentad-averaged columnar  $\delta\text{D}$  for the entire region. Averaged columnar  $\delta\text{D}$  for pre-monsoon (April and May) and monsoon (June–August) months was correlated with the rainfall data. Pearson correlation coefficient maps were generated between area-averaged columnar  $\delta\text{D}$  for pre-monsoon (April–May) and monsoon (June–August) months and grid-level total precipitation for the corresponding months. Contours were generated for those regions where correlation was significant ( $p < 0.05$ ). Correlation coefficient maps were also generated between grid-level ( $2^\circ \times 2^\circ$ ) mean-monthly columnar  $\delta\text{D}$  values and monthly Multivariate El-Niño Index (MEI). Monthly MEI was computed by taking mean of  $i$ th and  $(i - 1)$ th bi-monthly MEI values. Values were represented for significant correlations only, where  $p < 0.05$ . Methodology used in this paper has been summarized in the flow chart shown in figure 2.

## 4. Results

### 4.1 Temporal variability of columnar $\delta\text{D}$

Figure 3(a) represents the temporal variability of mean columnar  $\delta\text{D}$  over the study area (black line) along with standard deviation of all valid observations within a pentad (grey shaded region). From the figure, it is evident that columnar  $\delta\text{D}$  has a cyclic behavior. Fitting a simple second order Fourier series helps us visualize the two distinct frequency components: high  $\delta\text{D}$  values during summer season (owing to enriched vapor and reduction in fractionation factor) and sudden reduction in  $\delta\text{D}$  values with onset of monsoon during June. The values are low throughout winter months owing to lack of available moisture and increased fractionation factor at lower temperatures. From figure 3(b), the mean values range between  $-210\text{‰}$  during winter months (December–January) and  $-105\text{‰}$  during summer months (April–May). Although the inter-annual variability follows a distinct cyclic pattern, there are evident deviations from this trend during some years. These fluctuations or departures from mean can provide vital clues about the ongoing processes occurring in the region that affect the stable water isotope ratios in the atmosphere.

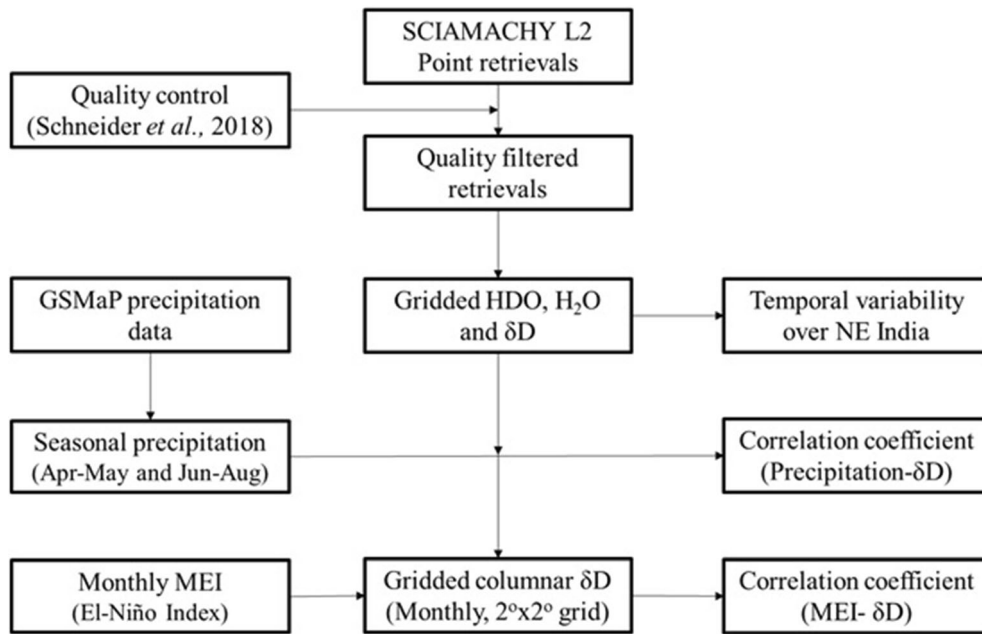


Figure 2. Flowchart of methodology used.

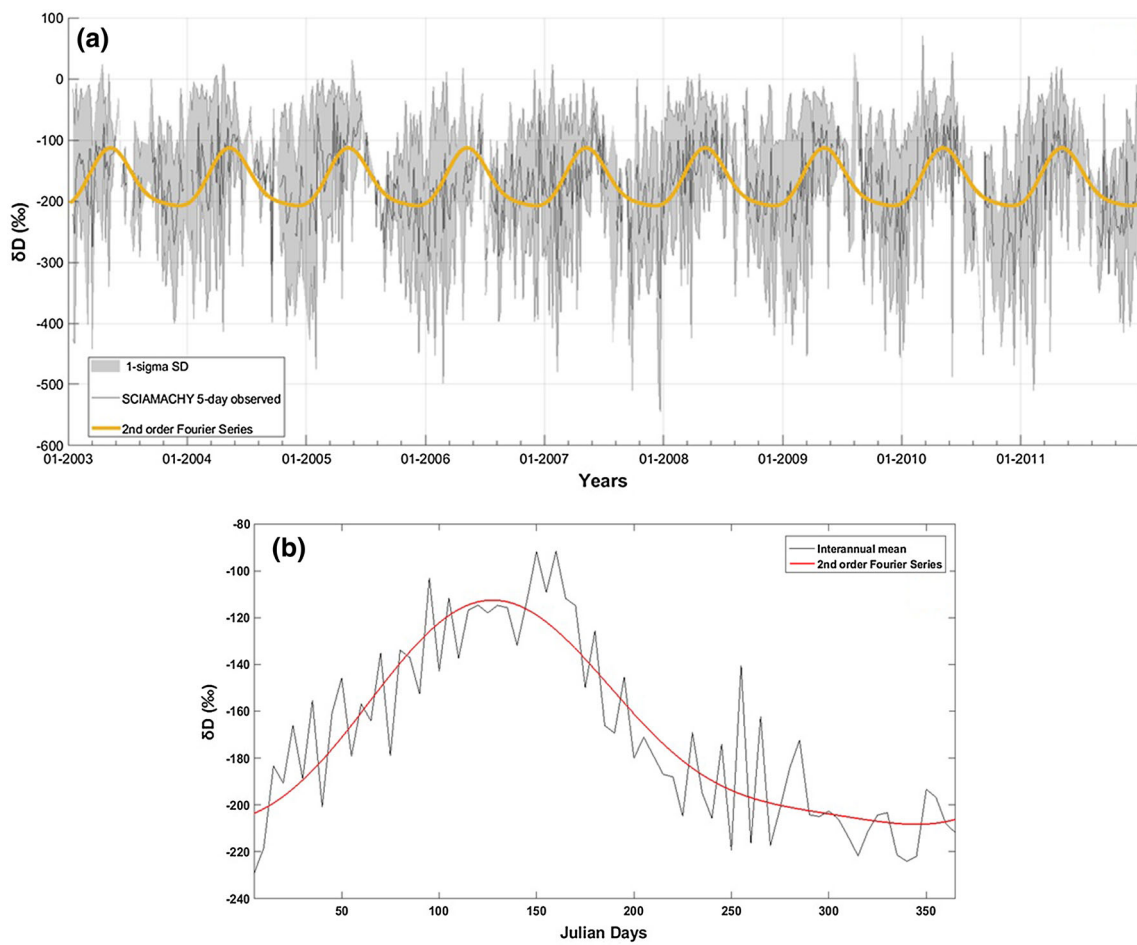


Figure 3. (a) Temporal variability of pentad averaged columnar  $\delta D$  over study area. Black line represents mean of all valid observations and shaded area represents one standard deviation. Yellow line is a simple second-order Fourier series fit. (b) Interannual mean over all pentads for 9 years (2003–2011).

#### 4.2 Relationship between $\delta D$ and precipitation

Precipitation occurs when vapor is removed from the atmosphere and since phase change influences water isotope ratios, precipitation plays a direct role in governing columnar  $\delta D$ . Heavier isotopes of water (like HDO) tend to condense rather easily and hence, the remaining vapor after precipitation is mostly depleted in heavy isotopes.  $\delta D$  values, along with specific humidity and temperature, provide valuable information about the source of vapor. To understand this linkage, we plot inter-annual  $\delta D$  during pre-monsoon (April–May) and monsoon (June–August) seasons with the mean seasonal precipitation during monsoon months (figure 4). From figure 4, it was observed that variability of  $\delta D$  during pre-monsoon season closely follows the trend in monsoon precipitation. During 2006, we see a reduction in water isotope ratios in both pre-monsoon and monsoon seasons and correspondingly lowest precipitation was observed in the region during this time. This trend, however, breaks in year 2011. Relationship between these two variables can be understood in detail using a grid-level analysis. Nevertheless, this figure does provide us with evidence of possible correlation between pre-monsoon isotope ratios and monsoon precipitation.

Since  $\delta D$  and precipitation were found to be inter-related, studying the spatial correlation between the two variables can reveal information about surface and lower atmospheric processes governing monsoonal precipitation. The aim of this analysis was to identify the areas where

monsoon precipitation is affected by water isotope ratios. This could also imply that the conditioning of atmosphere by surface processes (like evaporation, transpiration and moisture transport) during pre-monsoon season plays a vital role in governing the monsoon precipitation in those regions. With this basis, we computed Pearson correlation coefficients between area-averaged columnar  $\delta D$  (during pre-monsoon and monsoon) for the study region and the corresponding grid-level seasonal precipitation. Four maps representing the spatial distribution of correlation between these two variables were generated (figure 5). The regions where significant correlation ( $p < 0.05$ ) was observed have been represented with contours. Artifacts in GSMaP precipitation data resulted in spurious lines on the right side of these images.

From figure 5(a), we observe significant negative correlation between pre-monsoon  $\delta D$  and pre-monsoon precipitation over parts of central Bangladesh and West Bengal. This could be due to the fact that precipitation causes the remaining vapor to be depleted in heavier isotopes. Hence, these regions show a direct negative correlation between the two variables. From figure 5(b), we observe a positive correlation between pre-monsoon  $\delta D$  and monsoon precipitation over Meghalaya and parts of Assam. This region receives some of the highest rainfall in India and a positive correlation implies that the conditioning of atmosphere occurring during pre-monsoon season is linked with the amount of precipitation during monsoon season. This figure provides evidence that surface and

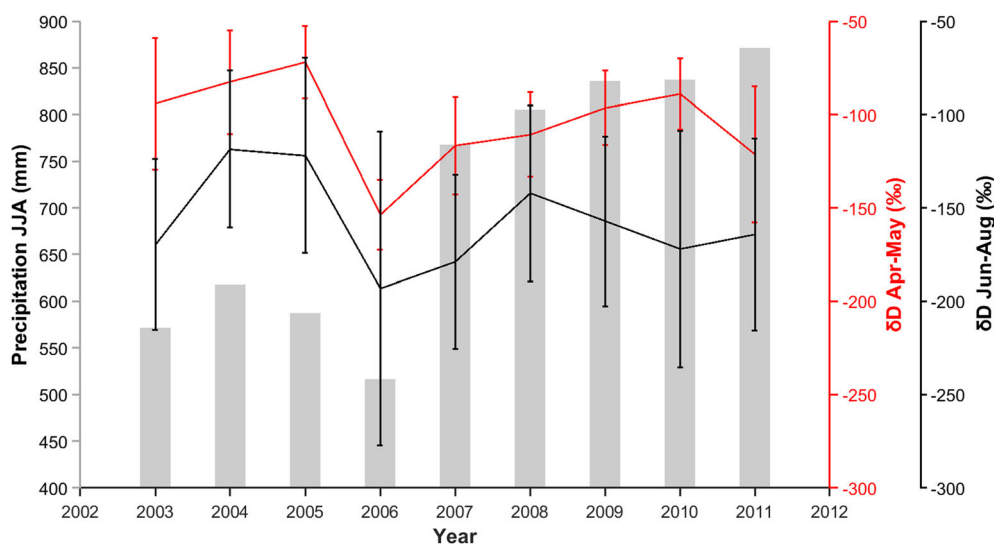


Figure 4. Inter-annual variability of water isotope ratios during pre-monsoon and monsoon season compared with average JJA precipitation for the corresponding year.

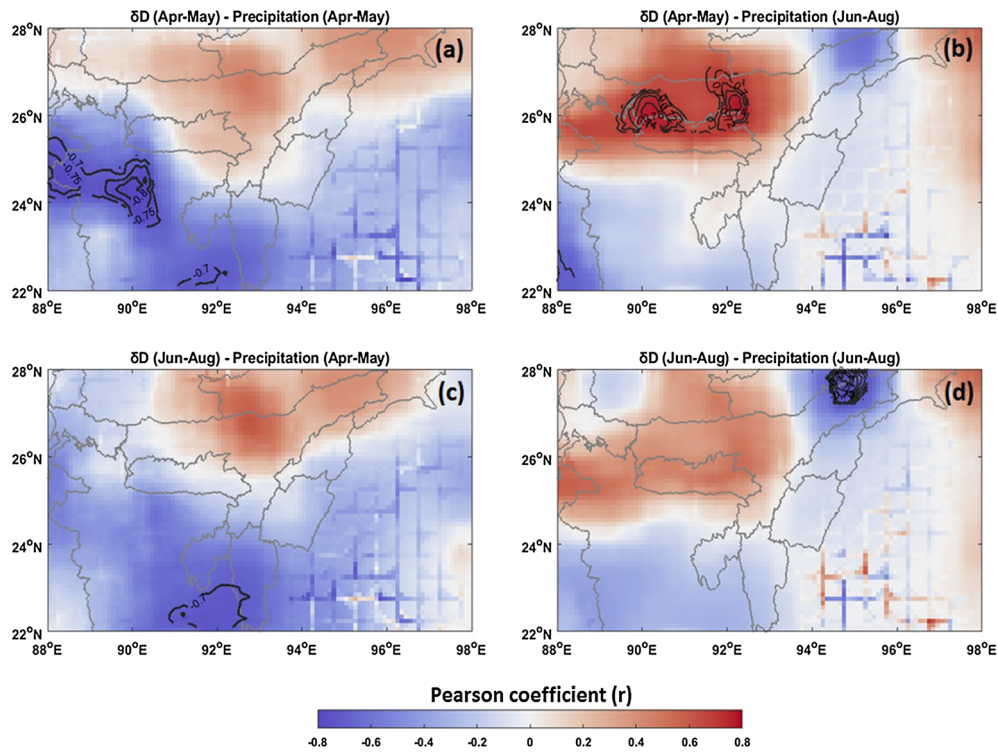


Figure 5. Pearson correlation coefficient ( $r$ ) between area-averaged columnar  $\delta D$  and grid-level seasonal precipitation for the study period. (a) pre-monsoon  $\delta D$  with pre-monsoon precipitation, (b) pre-monsoon  $\delta D$  with monsoon precipitation, (c) monsoon  $\delta D$  with pre-monsoon precipitation, and (d) monsoon  $\delta D$  with monsoon precipitation. Contours represent regions with significant correlation ( $p < 0.05$ ).

atmospheric processes affecting pre-monsoon water-isotope ratios in this region also govern monsoon rainfall. Evapotranspiration plays a crucial role in determining isotope ratios in the overlying atmosphere. On one hand, evaporation results in depleted water vapor and on the other, transpiration does not cause fractionation at steady state resulting in similar isotope ratios in vapor and liquid phase. An increase in pre-monsoon  $\delta D$  could signify enhanced evapotranspiration from this region and this could positively influence the monsoon precipitation.

### 4.3 Relationship between $\delta D$ and ENSO

Columnar isotope ratios are not only governed by local processes but also by global climate phenomenon such as ENSO, IOD etc. ENSO plays an important role in influencing global climate and different regions respond differently to these oscillations. Multivariate El-Niño Index (MEI) is a comprehensive quantification of ENSO phenomenon, which considers into account six different variables. Figure 6(a) represents regions

showing significant Pearson correlation coefficient ( $p < 0.05$ ) between monthly MEI and monthly columnar  $\delta D$  at  $2^\circ \times 2^\circ$  grids with zero-lag. Maximum correlation of 0.33 was observed between the two variables. Effect of ENSO on water isotope ratio was highest over central and southern India including Maharashtra, Chhattisgarh, Orissa, Telangana and Andhra Pradesh. Parts of Mizoram, Tripura, Bangladesh and West Bengal also showed weak correlation between the two variables indicating that the atmosphere in these regions responds to ENSO phenomenon within a month. Parts of Myanmar, Laos and central Thailand also show significant positive correlation with MEI due to their vicinity to the Pacific Ocean where ENSO occurs. Figure 6(b) shows the correlation coefficient where MEI lags  $\delta D$  by one month. The effect of ENSO was observed even after 1 month in same regions where peak correlation was seen with zero lag, however, these effects were greatly reduced. From figure 6(a, b), we can conclude that the atmosphere over these regions responds to ENSO within a month and it plays a role in influencing water isotope ratios.

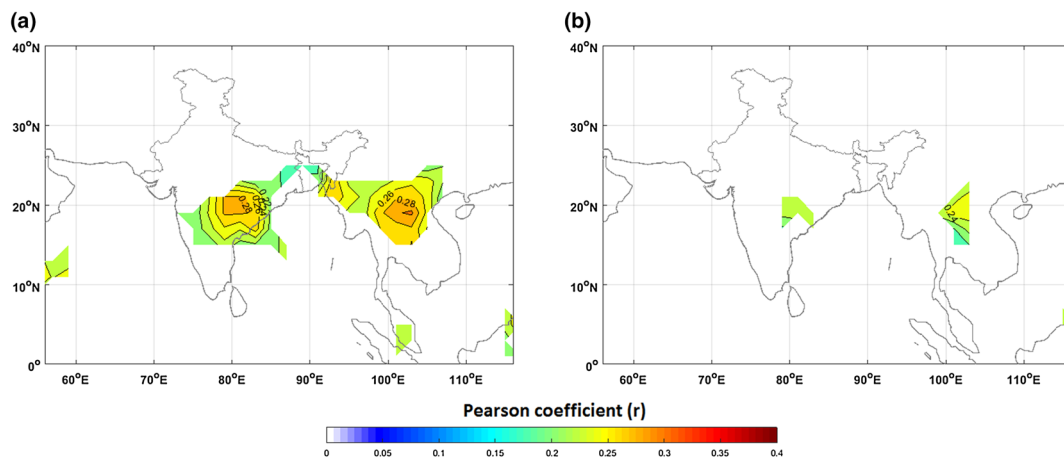


Figure 6. Pearson correlation coefficient between MEI and mean monthly columnar  $\delta D$  with (a) no lag and (b) 1 month lag. Only significant values ( $p < 0.05$ ) are represented.

## 5. Conclusion

In this paper, we discussed the relationship between monsoon precipitation and SCIAMACHY observed columnar water isotope ratios during pre-monsoon and monsoon seasons for Northeast India. Significant positive correlation ( $r > 0.7$ ,  $p < 0.05$ ) between  $\delta D$  and grid-level GSMaP precipitation was observed over parts of Meghalaya and central Assam, indicating strong correlation between pre-monsoon surface/atmospheric processes and amount of monsoon rainfall over the region. This finding may have implications in inclusion of water isotope ratios as an input parameter for various weather forecasting models. Effect of ENSO on water isotope ratios in atmosphere was studied and a positive correlation was observed between  $\delta D$  and MEI over parts of Central India, Myanmar, Laos and Thailand. Further study needs to be carried out to understand the variations in atmospheric water isotopes in response to declining monsoon precipitation over Northeast India.

## Acknowledgements

This work was carried out under SARITA program of Land Hydrology Division, EPSA, SAC, ISRO. The authors would like to thank Shri D K Das, Director SAC, Dr Raj Kumar, Deputy Director, EPSA and Dr A S Rajawat, Group Director, Geo-Sciences, Hydrosphere, Cryosphere Sciences and Applications Group (GHCAG) for providing us the opportunity to work on the subject. We are thankful to Global Rainfall Map (GSMaP) by JAXA Global Rainfall Watch for precipitation

information, NOAA for providing Multivariate El-Niño Index (MEI) and SRON for SCIAMACHY datasets.

## References

- Breitenbach S F M, Adkins J K, Meyer H, Marwan N, Kumar K K and Haug G H 2010 Strong influence of water vapor source dynamics on stable isotopes in precipitation observed in Southern Meghalaya, NE India; *Earth Planet. Sci. Lett.* **292(1–2)** 212–220.
- Dansgaard W 1964 Stable isotopes in precipitation; *Tellus* **16(4)** 436–468.
- Deshpande R D, Maurya A S, Kumar B, Sarkar A and Gupta S K 2010 Rain–vapor interaction and vapor source identification using stable isotopes from semiarid western India; *J. Geophys. Res.* **115** D23311, <https://doi.org/10.1029/2010JD014458>.
- Dikshit K R and Dikshit J K 2014 Natural vegetation: forests and grasslands of North-East India; In: *North-East India: Land, People and Economy, Advances in Asian Human-Environmental Research*, pp. 213–255, [https://doi.org/10.1007/978-94-007-7055-3\\_9](https://doi.org/10.1007/978-94-007-7055-3_9).
- Frankenberg C, Yoshimura K, Warneke T, Aben I, Butz A, Deutscher N, Griffith D, Hase F, Notholt J, Schneider M, Schrijver H and Röckmann T 2009 Dynamic processes governing lower-tropospheric HDO/H<sub>2</sub>O ratios as observed from space and ground; *Science* **325** 1374–1377.
- Friedl M A, Sulla-Menashe D, Tan B, Schneider A, Ramankutty N, Sibley A and Huang X 2010 *MODIS Collection 5 global land cover: Algorithm refinements and characterization of new datasets*; *Rem. Sens. Env.* **114(1)** 168–182
- Gat J R 1996 Oxygen and hydrogen isotopes in the hydrological cycle; *Annu. Rev. Earth Planet. Sci.* **24** 225–262.
- Guhathakurta P and Rajeevan M 2008 Trends in the rainfall pattern over India; *Int. J. Climatol.* **28** 1453–1469.
- Jain S K, Kumar V and Saharia M 2013 Analysis of rainfall and temperature trends in northeast India; *Int. J. Climatol.* **33** 968–978.



- Jeelani G, Deshpande R D, Galkowski M and Rozanski K 2018 Isotopic composition of daily precipitation along the southern foothills of the Himalayas: Impact of marine and continental sources of atmospheric moisture; *Atmos. Chem. Phys.* **18** 8789–8805, <https://doi.org/10.5194/acp-18-8789-2018>.
- Krishna Kumar K, Soman M K and Rupa Kumar K 1995 Seasonal forecasting of Indian summer monsoon rainfall: a review; *Weather* **50** 449–467.
- Laskar A H, Ramesh R, Burman J, Midhun M, Yadava M G, Jani R A and Gandhi N 2015 Stable isotopic characterization of Nor'westers of Southern Assam, NE India; *J. Clim. Change* **1(1–2)** 75–87, <https://doi.org/10.3233/JCC-150006>.
- Lee J E, Risi C, Fung I, Worden J, Scheepmaker R A, Lintner B and Frankenberg C 2012 Asian monsoon hydrometeorology from TES and SCIAMACHY water vapor isotope measurements and LMDZ simulations: Implications for speleothems climate record interpretation; *J. Geophys. Res.* **117** D15112, <https://doi.org/10.1029/2011JD017133>.
- Lekshmy P R, Midhun M and Ramesh R 2015 Spatial variation of amount effect over peninsular India and Sri Lanka: role of seasonality; *Geophys. Res. Lett.* **42** 5500–5507, <https://doi.org/10.1002/2015GL064517>.
- Mahanta R, Sarma D and Choudhury A 2013 Heavy rainfall occurrences in northeast India; *Int. J. Climatol.* **33** 1456–1469.
- Mook W G 2000 Environmental Isotopes in the Hydrological Cycle. Principles and Applications, *UNESCO/IAEA Series*, <http://www.naweb.iaea.org/naweb/ih/volumes.asp>.
- Nassar R, Bernath P F, Boone C D, Gettelman A, McLeod S D and Rinsland C P 2007 Variability in HDO/H<sub>2</sub>O abundance ratios in the tropical tropopause layer; *J. Geophys. Res.* **112(D21)** 305.
- Okazaki A, Satoh A, Tremoy G, Vimeux F, Scheepmaker R and Yoshimura K 2015 Interannual variability of isotopic composition in water vapor over western Africa and its relationship to ENSO; *Atmos. Chem. Phys.* **15** 3193–3204.
- Payne V H, Noone D, Dudhia A, Piccolo C and Grainger R G 2007 Global satellite measurements of HDO and implications for understanding the transport of water vapor into the stratosphere; *Q. J. R. Meteorol. Soc.* **133(627)** 1459–1471.
- Philander S G H 1983 Anomalous El Niño of 1982–1983; *Nature* **305** 16, <https://doi.org/10.1038/305016a0>.
- Prabhu A, Oh J, Kim I-W, Kripalani R H, Mitra A K and Pandithurai G 2017 Summer monsoon rainfall variability over North East regions of India and its association with Eurasian snow, Atlantic sea surface temperature and Arctic Oscillation; *Clim. Dyn.* **49(7–8)** 2545–2556, <https://doi.org/10.1007/s00382-016-3445-4>.
- Preethi B, Mujumdar M, Kripalani R H, Prabhu A and Krishnan R 2017 Recent trends and tele-connections among South and East Asian summer monsoons in a warming environment; *Clim. Dyn.* **48** 2489–2505, <https://doi.org/10.1007/s00382-016-3218-0>.
- Procter J, Haridasan K and Smith G W 1998 How far North does lowland evergreen tropical rain forest Go? *Glob. Ecol. Biogeogr. Lett.* **7(2)** 141–146, <https://doi.org/10.2307/2997817>.
- Scheepmaker R A, Frankenberg C, Galli A, Butz A, Schrijver H, Deutscher N M, Wunch D, Warneke T, Fally S and Aben I 2013 Improved water vapour spectroscopy in the 4174–4300 cm<sup>-1</sup> region and its impact on SCIAMACHY HDO/H<sub>2</sub>O measurements; *Atmos. Meas. Tech.* **6** 879–894.
- Schneider A, Borsdorff T, aan de Brugh J, Hu H and Landgraf J 2018 A full mission data set of HDO/H<sub>2</sub>O columns from SCIAMACHY 2.3 μm reflectance measurements; *Atmos. Meas. Tech.* **11** 3339–3350.
- Srivastava R, Ramesh R and Rao T N 2014 Stable isotopic differences between summer and winter monsoon rains over southern India; *J. Atmos. Chem.* **71(4)** 321–331, <https://doi.org/10.1007/s10874-015-9297-1>.
- Tyagi A, Hatwar H R and Pai D S (eds) 2009 *Monsoon 2009: A Report National Climate Centre*; Indian Meteorological Department, Pune.
- Vuille M and Werner M 2005 Stable isotopes in precipitation recording South American summer monsoon and ENSO variability: observations and model results; *Clim. Dyn.* **25** 401–413.
- Walker G T 1923 Correlation in seasonal variations of weather. VIII. A preliminary study of world-weather; *Mem. Indian Meteorol. Dep.* **24** 75–131.
- Wolter K and Timlin M S 1998 Measuring the strength of ENSO events: How does 1997/98 rank? *Weather* **53** 315–324.
- Worden J, Bowman K, Noone D, Beer R, Clough S, Eldering A, Fisher B, Goldman A, Gunson M, Herman R, Kulawik S S, Lampel M, Luo M, Osterman G, Rinsland C, Rodgers C, Sander S, Shephard M and Worden H 2006 Tropospheric Emission Spectrometer observations of the tropospheric HDO/H<sub>2</sub>O ratio: Estimation approach and characterization; *J. Geophys. Res.* **111** D16309.
- Worden J, Noone D and Bowman K 2007 Importance of rain evaporation and continental convection in the tropical water cycle; *Nature* **445** 528–532.